## The discovery of <sup>9</sup>N and the limits of existence of atomic nuclei

```
R.J. Charity, 1. Wylie, 2. S.M. Wang, 3.4 T.B. Webb, K.W. Brown, G. Cerizza, Z. Chajecki, J.M. Elson, J. Estee, D.E.M Hoff, S.A. Kuvin, W.G. Lynch, J. Manfredi, 2.* N. Michel, D. McNeel, P. Morfouace, W. Nazarewicz, C.D. Pruitt, C. Santamaria, S. Sweany, J. Smith, L.G. Sobotka, M.B. Tsang, and A.H. Wuosmaa, Department of Chemistry, Washington University, St. Louis, Missouri 63130, USA.

Begin and J. Louis, Missouri 63130, USA.

Begin and J. Louis, Missouri 63130, USA.

Key Laboratory of Nuclear Physics and Ion-beam Application (MOE),
Institute of Modern Physics, Fudan University, Shanghai 200433, China.

Shanghai Research Center for Theoretical Nuclear Physics, NSFC and Fudan University, Shanghai 200438, China.

Department of Physics, Washington University, St. Louis, Missouri 63130, USA.

Department of Physics, Western Michigan University, Kalamazoo, Michigan 49008, USA.

Department of Physics, University of Connecticut, Storrs, Connecticut 06269, USA.

Institute of Modern Physics, Chinese Academy of Sciences, Lanzhou 730000, China.

(Dated: November 1, 2022)
```

The boundaries of the Chart of Nuclides contain exotic isotopes that possess extreme proton-to-neutron asymmetries. Here we report on two of the most exotic proton-rich isotopes where at least one half of their constitute nucleons are unbound. While the ground state of  ${}^8\mathrm{C}$  is a resonance, its first excited state lies in the diffuse borderland between nuclear states and fleeting scattering features. Evidence for  ${}^9\mathrm{N}$ , with seven protons and two neutrons, is also presented. This extremely proton-rich system represents the first-known example of a ground-state five-proton emitter. The energies of these states are consistent with theoretical predictions of an open-quantum-system approach.

Nuclei with large imbalances between their constituent numbers of protons and neutrons can have exotic properties. The largest imbalances occur beyond the proton and neutron drip lines where the nuclear ground states (g.s.) are unbound. Because of the odd-even staggering of the drip lines induced by the nucleonic superfluidity, the shedding of unbound protons is usually terminated in an even-Z, particle-bound residue. Thus just beyond the proton drip line one is likely to find single-proton emitters for odd-Z isotopes and two-proton (2p) emitters for even-Z isotopes [1, 2]. Even further removed, one finds 3p and 4p emitters. Presently,  $^7$ B,  $^{13}$ F,  $^{17}$ Na, and  $^{31}$ K are known 3p emitters [3–6] and  $^8$ C and  $^{18}$ Mg have been observed to decay by emission of four protons [7, 8].

Moving outward past the drip lines, the decay widths of the low-lying states increase, eventually melting into an unresolvable continuum as their lifetimes become commensurate with typical reaction and single-particle timescales. Here, the very notion of the nuclear state becomes questionable as the timescales are too short to talk about the existence of a nucleus. Indeed as discussed in Ref. [9], if a collection of nucleons survives for less than about  $10^{-22}$  s, it should not be considered a nucleus. In this regime, the decay properties manifest themselves as scattering features rather than well-defined resonances. The maximum decay width at the boundary for  $A \approx 8$ , based on single-particle timescales, is of order  $\Gamma=3.5$  MeV [10].

The 4p emitter  $^8\mathrm{C}$  has one half of its nucleons in the continuum and the remainder constitutes an  $\alpha$ -cluster. The nucleus  $^9\mathrm{N}$  is even more extreme with an additional proton in the continuum, so it is hard to imagine that the

traditional concept of a nuclear state is well-established. On the other hand, insights can be gained from other unbound clusters of nucleons. Unlike the g.s. of <sup>8</sup>C, the dineutron is not a real resonance but an antibound state [11]. Here the attractive interaction between the two neutrons is just insufficient to produce a bound state, but the nearly-bound nature is manifested by enhanced n+nscattering just above threshold and strong final-state effects. The diproton is a subthreshold resonance [12, 13] and is formally neither an antibound state nor a resonance (though closer to the latter), and again manifests itself by enhanced scattering strength and final-state effects. While there have been some recent suggestions of a tetra-neutron resonance, what was observed [14, 15] may instead be a final-state effect [16, 17]. Similar situations might occur in the first excited state of <sup>8</sup>C and the g.s. of <sup>9</sup>N and <sup>9</sup>He as presented in this work.

The nucleus  $^9\mathrm{N}$  has three neutrons less than the lightest particle-bound nitrogen isotope  $^{12}\mathrm{N}$  and one more proton than  $^8\mathrm{C}$  into which it decays. The neighboring isotope  $^{10}\mathrm{N}$  has only been observed in three studies [18–20]. It has low-lying states which are single-proton resonances although their structure is not well established. Some indication as to the structure of  $^9\mathrm{N}$  can be gleaned from its mirror partner  $^9\mathrm{He}$  for which low-energy structures decay by the  $n+^8\mathrm{He}$  channel.

Particular interest in  ${}^{9}$ He is due to the parity inversion of the ground-state spin for odd N=7 isotones with large neutron excesses when the second  $s_{1/2}$  neutron single-particle orbital intrudes into the p shell [21]. Most studies agree that there is a  $1/2^{-}$  resonance  $\approx 1.2$  MeV above threshold for  ${}^{9}$ He (see Ref. [22]), but there is less

agreement about its width [22-24]. A number of studies find some  $1/2^+$  strength below this resonance [22, 24-27] although this strength in some studies in not sufficient to justify a notion of a state [24, 27, 28].

Experiment.—An  $E/A=69.5\,\mathrm{MeV}$  secondary beam of  $^{13}\mathrm{O}$  (4×10<sup>5</sup> pps, purity 80%) was produced from the Coupled Cyclotron Facility at the National Superconducting Cyclotron Laboratory at Michigan State University. Charged particles created in the interaction with a 1 mm-thick  $^9\mathrm{Be}$  target were detected in the High Resolution Array (HiRA) [29] consisting of 14 E- $\Delta E$  telescopes covering scattering angles from 2.1° to 12.4°. See Supplemental Material (SM) [30] for more details. States in  $^9\mathrm{N}$  ( $^8\mathrm{C}$ ) were produced by knocking out 3 neutrons and 1 (2) protons from the projectile and identified using the invariant-mass technique. Data from this experiment pertaining to the first observation of  $^{11}\mathrm{O}$  [31, 32] and  $^{13}\mathrm{F}$  [4] as well as other previously-known isotopes [33–35] have already been published.

Invariant-Mass Spectra.— The detected  $4p+\alpha$  events have significant contamination from  $^{12}O\rightarrow 4p+2\alpha$  events where only one of the two  $\alpha$  particles are detected. The subtraction of this background in the four-proton decayenergy  $(Q_{4p})$  distribution of  ${}^{8}C$  is discussed in SM. The resulting background-subtracted distribution in Fig. 1(a) displays a broad structure at  $Q_{4p} \sim 7$  MeV in addition to the <sup>8</sup>C g.s. peak at 3.5 MeV. Of the possible intermediate states in the decay of <sup>8</sup>C, only the <sup>6</sup>Be g.s. resonance can be easily observed in the decay correlations because of its relatively narrow decay width. Its magnitude, as a function of  $Q_{4p}$ , is obtained from fitting this resonance in the invariant-mass spectrum of the  $2p+\alpha$  subevents (see SM). This gated <sup>8</sup>C distribution [Fig. 1(b)] has similar peak structures to the ungated version, but the background under the  $Q_{4p} \sim 7$  MeV feature, and at higher energies, has been significantly reduced.

The decay-energy  $(Q_{5p})$  distribution from all detected  $5p+\alpha$  events is quite wide and contains no prominent "narrow" peaks. However the distribution gated on a narrow intermediate state (both panels of Fig. 2) reduces the structureless background similar to that found for the  $4p+\alpha$  events. In this case, we have gated on the <sup>8</sup>C intermediate state which restricts the resulting distribution to  $Q_{5p} < 10$  MeV (see SM for details). This final distribution appears to have two peaks and thus may be a doublet rather than a singlet although the statistics is marginal for this distinction.

Theoretical models.— Since continuum effects are strong for both <sup>8</sup>C and <sup>9</sup>N, we used the complex-energy Gamow Shell Model (GSM) to determine the theoretical location of the nuclear states of interest as it has been used to study many weakly-bound and unbound systems [36–38] including the g.s. of <sup>8</sup>C [39]. GSM differs from the traditional closed-quantum-system nuclear shell model as it allows for bound, scattering, and Gamow resonant states to be treated on equal footing by imple-

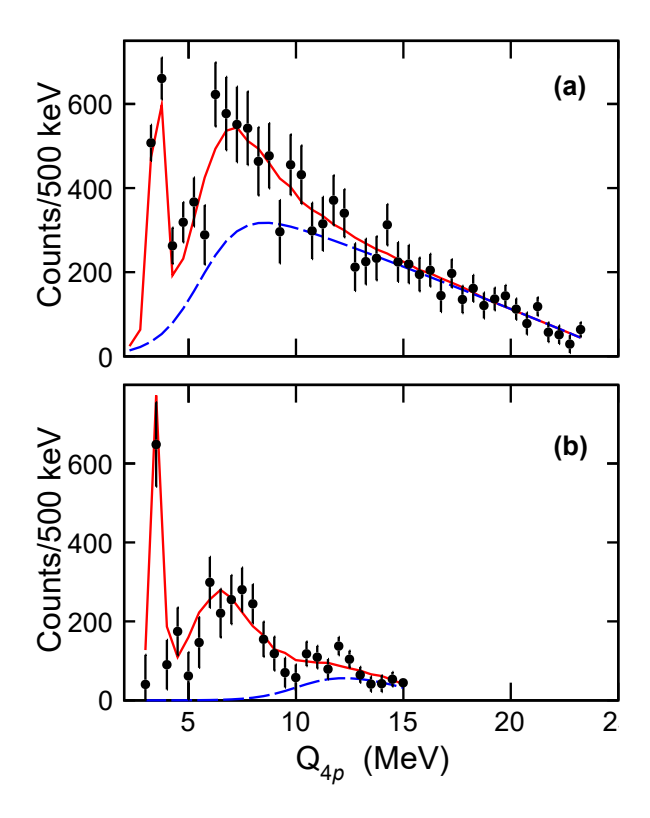


FIG. 1. Invariant-mass spectra for <sup>8</sup>C. (a) contamination-subtracted decay-energy spectrum for all <sup>8</sup>C fragments. (b) contamination-subtracted distribution where the decay involves a <sup>6</sup>Be intermediate state. The red curves show fits to these distribution assuming two peaks and a smooth background (blue dashed curves).

menting the Berggren basis.

Calculations for  $^8\mathrm{C}$  and  $^9\mathrm{N}$  were performed by assuming an  $\alpha$  core surrounded by four and five valence protons, respectively. We used the same valence-space Hamiltonian as described in previous GSM studies [39–41] with the parameters given in SM. The GSM predictions for experimentally determined states are presented in Fig. 3, with the predicted low-lying states tabulated in SM.

The properties of the low-lying states in  $^9$ N were crosschecked by the Gamow-Coupled-Channel (GCC) method [42], which is a three-body framework utilizing the Berggren ensemble. Based on a large proton-decaying branching ratio and spectroscopic factor ( $S_{s_{1/2}}^2 = 0.87$  and  $S_{p_{1/2}}^2 = 0.80$  according to GSM calculations),  $^9$ N can be described as a  $^8$ C+p two-body system. To investigate the decay properties, the low-lying states obtained by GCC were propagated using a time-dependent framework [43].

Discussion.— The GSM calculations predict the  $2^+$  first excited state of  $^8$ C at energy  $\approx 8.3$  MeV while an alternative approach using the complex-scaling technique predicts a value of 6.4 MeV [44]. The broad structure seen in both  $^8$ C decay-energy spectra of Fig. 1(a) and

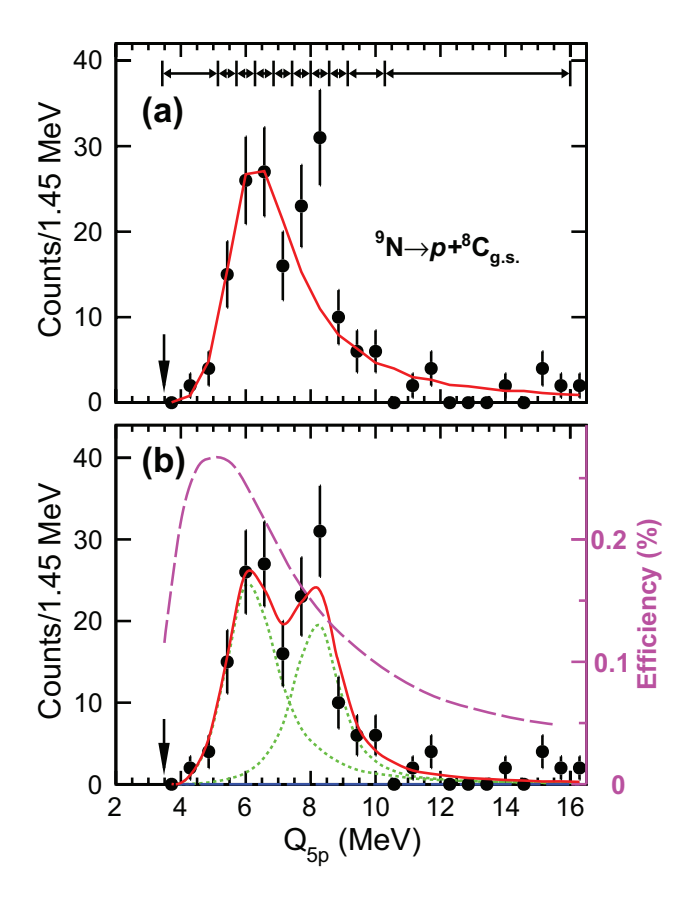


FIG. 2. Fits to the selected  $p+^8\mathrm{C}$  g.s. distribution. (a) Fit with a single-peak parameterized by an R-matrix lineshape. The fitting was made to the integrated yield in the ten bins shown at the top of this panel. (b) A two-peak fit where the upper peak mean energy and width are set to the GSM predictions for the  $J^{\pi}=1/2^-$  state of  $^9\mathrm{N}$ . The green dotted curves show contributions from each peak. The dependence of the detection efficiency as a function of  $Q_{5p}$  as determined in our Monte Carlo simulations (see SM) is shown by the dashed-magenta curve. In both panels, the  $p+^8\mathrm{C}$  g.s. threshold is indicated by an arrow.

1(b) peaks roughly in between these values and thus is a candidate for the  $2^+$  state. As this structure is present when there is a  $^6$ Be intermediate state, then its decay is similar to the g.s. in that it decays by two sequences of 2p decay [3].

The spectra in Fig. 1 were jointly fit each with two peaks (g.s. and 2<sup>+</sup>) where the broad asymmetric line-shape for the 2<sup>+</sup> state was taken for diproton emission to <sup>6</sup>Be in the *R*-matrix formulation assuming zero relative energy of the two protons [45]. These shapes were convoluted with the experimental resolution (see SM) and they were assumed to sit atop smooth backgrounds. Other lineshapes could be considered, but the largest source of uncertainty comes rather from the parameterization of the background and the low statistics. In terms of quantities that are less dependent on the line-shape parameterization, the maximum of the 2<sup>+</sup> lineshape occurs

at E = 7.1(1.1) MeV and its FWHM is 4.5(1.1) MeV.

With such a large width, the  $2^+$  state is located in the diffuse borderland between a true resonance and a scattering feature. The fitted width is in better agreement with the complex-scaling value of 4.3 MeV than the smaller value of  $\sim 1.5$  MeV from the GSM. In the complex-scaling calculations, other excited states are all significantly wider and they could possibly contribute to the smooth background at higher energy. On the other hand, the GSM model predicts some narrower excited states. There is a suggestion of an experimental peak at  $E \approx 12$  MeV in Fig. 1(b). This possible peak could be a  $3^-$  state predicted at  $\approx 13$  MeV in the GSM.

Moving on to  ${}^9\mathrm{N}$ , the  $Q_{5p}$  distribution for the selected  $p+{}^8\mathrm{C}(\mathrm{g.s.})$  events was fit assuming both a singlet and a doublet. The theory behind minimizing  $\chi^2$  requires that the errors for each data point are associated with a normal distribution [46]. This is not the case for the low and high-energy tails of our distribution where there are only a couple of counts in each bin and the statistics are described by Poisson distributions. We have therefore followed the advice of Ref. [46] and made the bin sizes larger in these tail regions to increase the counts. The 10 bins used in the fitting are shown at the top of Fig. 2(a) and we fit the integrated yields in these bins, but for display purposes, we still show the data and the fit using the original constant bin size in Fig. 2.

While the quality of a fit is often judged from the reduced  $\chi^2$ , this quantity is not defined in a non-linear fit [47] such as the present case. Rather we note that in a good fit, the deviations of the data points from their fitted values relative to their standard error should follow a standard normal distribution (mean=0, variance=1) [47]. This can be gauged with the Anderson-Darling test [48] where the resultant p-value takes values from zero (bad fit) to unity (good fit). Fits can be rejected at the 1-p confidence level.

Figure 2(b) shows an example of a two-peak fit of high quality with a p value of 95%. Here, the R-matrix parameters of the  $1/2^-$  peak are adjusted so that its S-matrix pole is consistent with the GSM prediction. With this constraint, the fitted values for the  $1/2^+$  strength are  $Q_{1p}{=}2.50(21)$  MeV  $[Q_{5p}{=}5.98(21)$  MeV] and  $\Gamma{=}1.81(53)$  MeV in excellent agreement with the GSM predictions of  $Q_{5p}{=}5.56$  MeV and  $\Gamma{=}1.74$  MeV. Another fit was made with the same  $1/2^-$  lineshape but with the  $J^{\pi}{=}1/2^+$  strength described by the GCC lineshape as a sub-threshold resonance. The fit (Fig. S4(b) in SM) is not as good with p=42% but cannot be totally discarded.

The presented two-peak fit in Fig. 2(b) is not unique and multiple R-matrix solutions lie along a long-narrow  $\chi^2$  valley in fitting-parameter space where the intrinsic widths of the  $1/2^+$  and  $1/2^-$  peaks are strongly anticorrelated and cannot be individually constrained. However, the peak energies from the poles of their S-

matrices are well constrained with  $Q_{5p}(1/2^+)=6.0(1)$  and  $Q_{5p}(1/2^-)=8.1(1)$  MeV in agreement with predictions. In all two-peak fits, the  $1/2^+$  state is a true resonance ( $\theta < 45^\circ$ , see inset of Fig. 4 for definition), however GCC subthreshold line shapes can also reproduce the  $1/2^+$  strength at reduced probabilities.

The consistency with the GSM predictions adds credence to the two-peak fits, but there is still the possibility, at lower probability, that we observed a singlepeak structure. In the R-matrix parameterization only an  $\ell=0$  resonance is capable of reproducing the width of the observed structure. The best single-peak fit, shown in Fig. 2(a), looks reasonable apart from one data point at  $Q_{5p} \approx 8.2$  MeV which is  $3.2 \sigma$  from its fitted value. The quality of this fit is characterized by a p-value of 38% which does not allow us to reject it with total confidence. From the fit, the pole of the  $p+{}^{8}$ C S-matrix is determined at  $Q_{1p}=1.22(16)$  MeV and  $\Gamma=2.59(23)$  MeV  $(\theta=23^{\circ})$ . Such a wide  $1/2^{+}$  level is approaching the diffuse borderland region for a real resonance. We have also considered fitting the data with a single subthreshold lineshape described by the GCC model, but this is largely rejected with p=7.3% (Fig. S4(a) in SM).

To provide insights into the nature of the  $1/2^+$  state in  $^9\mathrm{N}$ , GSM calculations were performed for its mirror partner,  $^9\mathrm{He}$ , using the same Hamiltonian parameters. Figure 3 shows the experimental spectrum is reproduced. While previous studies using the Berggren basis have indicated that the  $1/2^+$  state in  $^9\mathrm{He}$  is a resonance [40, 49], these calculations introduced some artificial binding to stabilize their results due to the choice of the basis (see SM for details). When the continuum effect is properly taken into account with a deformed scattering contour [50], one can generate an antibound  $1/2^+$  pole in  $^9\mathrm{He}$ , which has the best agreement with experimental data.

Although it is not possible for antibound poles to emerge in proton-rich nuclei due to the Coulomb interaction [42], we followed the same procedure as in  $^9{\rm He}$  to determine if the  $1/2^+$  state in  $^9{\rm N}$  is a resonance or subthreshold resonance. The predicted  $1/2^+$  state has an energy of E=2.08 MeV above the  $^8{\rm C}+p$  threshold and  $\Gamma=1.74$  MeV which indicates a proper resonance state. It must be noted, however, that the  $1/2^+$  state in GSM is very fragile with respect to changes of the Hamiltonian and the Berggren basis, so we cannot with certainty rule out a subthreshold resonance.

To pin down the very nature of the  $1/2^+$  structure in  $^9\mathrm{N}$ , more experimental studies are needed. Although, as shown above, it is difficult to distinguish a scattering feature from a proper resonance through spectrum or cross-section analysis, the time-dependent survival probability, as a physical observable, offers a way. As shown in Fig. 4, a proper resonance (the  $1/2^-$  state) usually would first decay exponentially, and then transition to a power-law decay due to the non-resonant continuum component [51, 52]. However, as the analog of the s-wave virtual

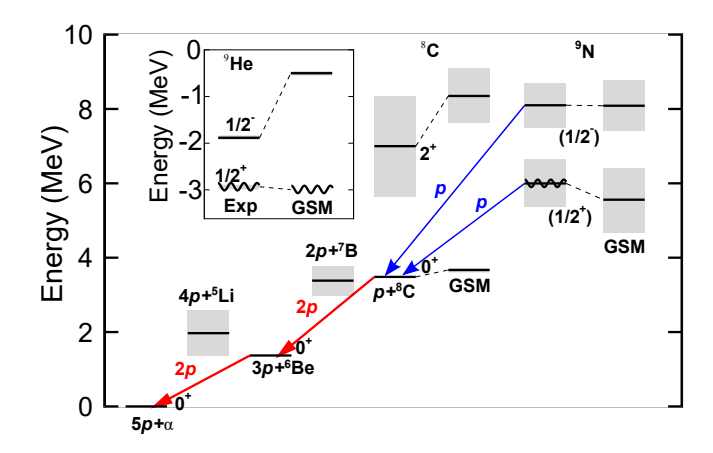


FIG. 3. Level diagrams of  $^8\mathrm{C}$  and  $^9\mathrm{N}$  obtained experimentally and calculated with the GSM. Energies are given relative to the  $^4\mathrm{He}$  threshold. The level diagram of  $^9\mathrm{He}$ , a mirror partner of  $^9\mathrm{N}$ , is shown in the inset. The  $1/2^+$  antibound state in  $^9\mathrm{He}$  is shown with a wavy line to indicate its status more as a scattering feature rather than a real state. The proposed  $1/2^+$  state in  $^9\mathrm{N}$  is shown with both straight and wavy lines to indicate the uncertainty as to its nature (a resonance or scattering feature) while the GSM interprets it as a resonance.

state, the  $1/2^+$  state of  $^9\mathrm{N}$  starts to depart from the exponential decay from the beginning when approaching the subthreshold region ( $\theta > 45^\circ$ ). In this case, the strong continuum component reveals the structure as a scattering feature. A measurement of the survival probability, however, represents an appreciable challenge for experiment due to the short lifetimes and very low production rates of nuclei located in the extremely proton-rich region of nuclear landscape.

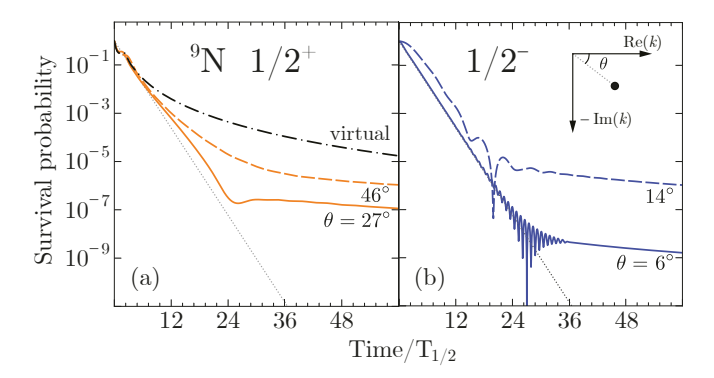


FIG. 4. Survival probabilities for  $^9\mathrm{N}$  levels as functions of time calculated for (a)  $1/2^+$  and (b)  $1/2^-$  states. The calculations were carried out with the GCC model with the depth  $V_0$  of the Woods-Saxon potential varied between  $-64\,\mathrm{MeV}$  (solid line) to  $-54\,\mathrm{MeV}$  (dashed line).  $\theta$  is the polar angle of the pole in the complex momentum k-plane. The dotted lines indicate the exponential-decay lineshape at short times. Also shown is the survival probability for the virtual  $1/2^+$  state (dash-dotted line; the time unit  $\mathrm{T}_{1/2}$  is taken as  $40\,\mathrm{fm}/c)$ .

Both <sup>8</sup>C and <sup>9</sup>N shed their excess protons by a se-

ries of single-proton and prompt 2p decays. The 4p-emitter  $^{18}$ Mg also decays in this manner [8], suggesting this behavior is typical for isotopes at the limits of existence. Our analysis suggest that some observed structures, sometimes interpreted in terms of nuclear states, should be rather viewed as fleeting features lying outside the Chart of Nuclides.

Conclusions.— We have made the first observation of the nuclide <sup>9</sup>N produced from multi-nucleon knockout from a <sup>13</sup>O beam. The invariant-mass spectrum of detected  $5p+\alpha$  events each containing an  ${}^{8}\mathrm{C}$  g.s. as intermediate state displays a structure which can be interpreted as two peaks, although a single peak solution cannot be total discounted. This nuclide has also been studied theoretically in the Gamow Shell Model where the important effects of the continuum are included. The predicted location and widths of the  $1/2^+$  and  $1/2^-$  resonances are in excellent agreement with experimental result giving further evidence for the preferred two-peak solution. The  $1/2^+$  resonance, the mirror of an antibound state in <sup>9</sup>He, is most likely a true resonance rather than a subthreshold resonance, but the latter is not completely ruled out in both the experiment and in theory. The  $2^+$ state in the neighboring nuclide <sup>8</sup>C has also been investigated in the same experiment. Its width is very wide  $\Gamma$ =4.5(1.1) MeV which puts it at the borderland between a real resonance and a scattering feature.

This material is based upon work supported by the U.S. Department of Energy, Office of Science, Office of Nuclear Physics under Awards No. DE-FG02-87ER-40316, No. DE-FG02-04ER-41320, No. DE-SC0014552, DOE-DE-SC0013365, DE-SC0023175, the National Science Foundation under Grant No. PHY- 156556, and the National Natural Science Foundation of China under Grant Nos. 12175281. J. M. was supported by a Department of Energy National Nuclear Security Administration Steward Science Graduate Fellowship under cooperative agreement No. DE- NA0002135.

- \* Present address: Department of Engineering Physics, Air Force Institute of Technology, Wright-Patterson AFB, Ohio
- M. Pfützner, M. Karny, L. V. Grigorenko, and K. Riisager, Radioactive decays at limits of nuclear stability, Rev. Mod. Phys. 84, 567 (2012).
- [2] L. Neufcourt, Y. Cao, S. Giuliani, W. Nazarewicz, E. Olsen, and O. B. Tarasov, Beyond the proton drip line: Bayesian analysis of proton-emitting nuclei, Phys. Rev. C 101, 014319 (2020).
- [3] R. J. Charity, J. M. Elson, J. Manfredi, R. Shane, L. G. Sobotka, B. A. Brown, Z. Chajecki, D. Coupland, H. Iwasaki, M. Kilburn, J. Lee, W. G. Lynch, A. Sanetullaev, M. B. Tsang, J. Winkelbauer, M. Youngs, S. T. Marley, D. V. Shetty, A. H. Wuosmaa, T. K. Ghosh, and M. E. Howard, Investigations of three-, four-, and five-

- particle decay channels of levels in light nuclei created using a  $^9\mathrm{C}$  beam, Phys. Rev. C 84, 014320 (2011).
- [4] R. J. Charity, T. B. Webb, J. M. Elson, D. E. M. Hoff, C. D. Pruitt, L. G. Sobotka, K. W. Brown, G. Cerizza, J. Estee, W. G. Lynch, J. Manfredi, P. Morfouace, C. Santamaria, S. Sweany, C. Y. Tsang, M. B. Tsang, Y. Zhang, K. Zhu, S. A. Kuvin, D. McNeel, J. Smith, A. H. Wuosmaa, and Z. Chajecki, Observation of the exotic isotope <sup>13</sup>F located four neutrons beyond the proton drip line, Phys. Rev. Lett. 126, 132501 (2021).
- [5] K. W. Brown, R. J. Charity, J. M. Elson, W. Reviol, L. G. Sobotka, W. W. Buhro, Z. Chajecki, W. G. Lynch, J. Manfredi, R. Shane, R. H. Showalter, M. B. Tsang, D. Weisshaar, J. R. Winkelbauer, S. Bedoor, and A. H. Wuosmaa, Proton-decaying states in light nuclei and the first observation of <sup>17</sup>Na, Phys. Rev. C 95, 044326 (2017).
- [6] D. Kostyleva, I. Mukha, L. Acosta, E. Casarejos, V. Chudoba, A. A. Ciemny, W. Dominik, J. A. Dueñas, V. Dunin, J. M. Espino, A. Estradé, F. Farinon, A. Fomichev, H. Geissel, A. Gorshkov, L. V. Grigorenko, Z. Janas, G. Kamiński, O. Kiselev, R. Knöbel, S. Krupko, M. Kuich, Y. A. Litvinov, G. Marquinez-Durán, I. Martel, C. Mazzocchi, C. Nociforo, A. K. Ordúz, M. Pfützner, S. Pietri, M. Pomorski, A. Prochazka, S. Rymzhanova, A. M. Sánchez-Benítez, C. Scheidenberger, H. Simon, B. Sitar, R. Slepnev, M. Stanoiu, P. Strmen, I. Szarka, M. Takechi, Y. K. Tanaka, H. Weick, M. Winkler, J. S. Winfield, X. Xu, and M. V. Zhukov, Towards the limits of existence of nuclear structure: Observation and first spectroscopy of the isotope <sup>31</sup>K by measuring its three-proton decay, Phys. Rev. Lett. 123, 092502 (2019).
- [7] R. J. Charity, J. M. Elson, J. Manfredi, R. Shane, L. G. Sobotka, Z. Chajecki, D. Coupland, H. Iwasaki, M. Kilburn, J. Lee, W. G. Lynch, A. Sanetullaev, M. B. Tsang, J. Winkelbauer, M. Youngs, S. T. Marley, D. V. Shetty, A. H. Wuosmaa, T. K. Ghosh, and M. E. Howard, 2p-2p decay of <sup>8</sup>C and isospin-allowed 2p decay of the isobaricanalog state in <sup>8</sup>B, Phys. Rev. C 82, 041304 (2010).
- [8] Y. Jin, C. Y. Niu, K. W. Brown, Z. H. Li, H. Hua, A. K. Anthony, J. Barney, R. J. Charity, J. Crosby, D. Dell'Aquila, J. M. Elson, J. Estee, M. Ghazali, G. Jhang, J. G. Li, W. G. Lynch, N. Michel, L. G. Sobotka, S. Sweany, F. C. E. Teh, A. Thomas, C. Y. Tsang, M. B. Tsang, S. M. Wang, H. Y. Wu, C. X. Yuan, and K. Zhu, First observation of the four-proton unbound nucleus <sup>18</sup>Mg, Phys. Rev. Lett. 127, 262502 (2021).
- [9] M. Thoennessen, Reaching the limits of nuclear stability, Rep. Prog. Phys. 67, 1187 (2004).
- [10] K. Fossez, W. Nazarewicz, Y. Jaganathen, N. Michel, and M. Płoszajczak, Nuclear rotation in the continuum, Phys. Rev. C 93, 011305 (2016).
- [11] H. C. Ohanian and C. G. Ginsburg, Antibound 'states' and resonances, Am. J. Phys. 42, 310 (1974).
- [12] L. P. Kok, Accurate determination of the ground-state level of the <sup>2</sup>He nucleus, Phys. Rev. Lett. 45, 427 (1980).
- [13] A. M. Mukhamedzhanov, B. F. Irgaziev, V. Z. Goldberg, Y. V. Orlov, and I. Qazi, Bound, virtual, and resonance S-matrix poles from the Schrödinger equation, Phys. Rev. C 81, 054314 (2010).
- [14] K. Kisamori, S. Shimoura, H. Miya, S. Michimasa, S. Ota, M. Assie, H. Baba, T. Baba, D. Beaumel, M. Dozono, T. Fujii, N. Fukuda, S. Go, F. Hammache, E. Ideguchi, N. Inabe, M. Itoh, D. Kameda, S. Kawase, T. Kawabata, M. Kobayashi, Y. Kondo,

- T. Kubo, Y. Kubota, M. Kurata-Nishimura, C. S. Lee, Y. Maeda, H. Matsubara, K. Miki, T. Nishi, S. Noji, S. Sakaguchi, H. Sakai, Y. Sasamoto, M. Sasano, H. Sato, Y. Shimizu, A. Stolz, H. Suzuki, M. Takaki, H. Takeda, S. Takeuchi, A. Tamii, L. Tang, H. Tokieda, M. Tsumura, T. Uesaka, K. Yako, Y. Yanagisawa, R. Yokoyama, and K. Yoshida, Candidate resonant tetraneutron state populated by the <sup>4</sup>He(<sup>8</sup>He, <sup>8</sup>Be) reaction, Phys. Rev. Lett. **116**, 052501 (2016).
- [15] M. Duer et al., Observation of a correlated free fourneutron system, Nature 606, 678 (2022).
- [16] A. Deltuva, Tetraneutron: Rigorous continuum calculation, Phys. Lett. B 782, 238 (2018).
- [17] M. D. Higgins, C. H. Greene, A. Kievsky, and M. Viviani, Nonresonant density of states enhancement at low energies for three or four neutrons, Phys. Rev. Lett. 125, 052501 (2020).
- [18] A. Lépine-Szily, J. M. Oliveira, V. R. Vanin, A. N. Ostrowski, R. Lichtenthäler, A. Di Pietro, V. Guimarães, A. M. Laird, L. Maunoury, G. F. Lima, F. de Oliveira Santos, P. Roussel-Chomaz, H. Savajols, W. Trinder, A. C. C. Villari, and A. de Vismes, Observation of the particle-unstable nucleus <sup>10</sup>N, Phys. Rev. C 65, 054318 (2002).
- [19] J. Hooker, G. Rogachev, V. Goldberg, E. Koshchiy, B. Roeder, H. Jayatissa, C. Hunt, C. Magana, S. Upadhyayula, E. Uberseder, and A. Saastamoinen, Structure of <sup>10</sup>N in <sup>9</sup>C+p resonance scattering, Phys. Lett. B **769**, 62 (2017).
- [20] R. J. Charity, T. B. Webb, L. G. Sobotka, and K. W. Brown, Spectroscopy of <sup>10</sup>N with the invariant-mass method, Phys. Rev. C 104, 054307 (2021).
- [21] T. Aumann, A. Navin, D. P. Balamuth, D. Bazin, B. Blank, B. A. Brown, J. E. Bush, J. A. Caggiano, B. Davids, T. Glasmacher, V. Guimarães, P. G. Hansen, R. W. Ibbotson, D. Karnes, J. J. Kolata, V. Maddalena, B. Pritychenko, H. Scheit, B. M. Sherrill, and J. A. Tostevin, One-neutron knockout from individual single-particle states of <sup>11</sup>Be, Phys. Rev. Lett. 84, 35 (2000).
- [22] T. Al Kalanee, J. Gibelin, P. Roussel-Chomaz, N. Keeley, D. Beaumel, Y. Blumenfeld, B. Fernández-Domínguez, C. Force, L. Gaudefroy, A. Gillibert, J. Guillot, H. Iwasaki, S. Krupko, V. Lapoux, W. Mittig, X. Mougeot, L. Nalpas, E. Pollacco, K. Rusek, T. Roger, H. Savajols, N. de Séréville, S. Sidorchuk, D. Suzuki, I. Strojek, and N. A. Orr, Structure of unbound neutronrich <sup>9</sup>He studied using single-neutron transfer, Phys. Rev. C 88, 034301 (2013).
- [23] H. G. Bohlen, B. Gebauer, D. Kolbert, W. von Oertzen, E. Stiliaris, M. Wilpert, and T. Wilpert, Spectroscopy of <sup>9</sup>He with the (<sup>13</sup>C, <sup>13</sup>O)-reaction on <sup>9</sup>Be, Z. Phys. A 330, 227 (1988).
- [24] D. Votaw, P. A. DeYoung, T. Baumann, A. Blake, J. Boone, J. Brown, D. Chrisman, J. E. Finck, N. Frank, J. Gombas, P. Guèye, J. Hinnefeld, H. Karrick, A. N. Kuchera, H. Liu, B. Luther, F. Ndayisabye, M. Neal, J. Owens-Fryar, J. Pereira, C. Persch, T. Phan, T. Redpath, W. F. Rogers, S. Stephenson, K. Stiefel, C. Sword, A. Wantz, and M. Thoennessen, Low-lying level structure of the neutron-unbound N = 7 isotones, Phys. Rev. C 102, 014325 (2020).
- [25] L. Chen, B. Blank, B. Brown, M. Chartier, A. Galonsky, P. Hansen, and M. Thoennessen, Evidence for an l=0 ground state in <sup>9</sup>He, Phys. Lett. B 505, 21 (2001).

- [26] M. S. Golovkov, L. V. Grigorenko, A. S. Fomichev, A. V. Gorshkov, V. A. Gorshkov, S. A. Krupko, Y. T. Oganessian, A. M. Rodin, S. I. Sidorchuk, R. S. Slepnev, S. V. Stepantsov, G. M. Ter-Akopian, R. Wolski, A. A. Korsheninnikov, E. Y. Nikolskii, V. A. Kuzmin, B. G. Novatskii, D. N. Stepanov, P. Roussel-Chomaz, and W. Mittig, New insight into the low-energy <sup>9</sup>He spectrum, Phys. Rev. C 76, 021605 (2007).
- [27] H. Johansson, Y. Aksyutina, T. Aumann, K. Boretzky, M. Borge, A. Chatillon, L. Chulkov, D. Cortina-Gil, U. Datta Pramanik, H. Emling, C. Forssén, H. Fynbo, H. Geissel, G. Ickert, B. Jonson, R. Kulessa, C. Langer, M. Lantz, T. LeBleis, K. Mahata, M. Meister, G. Münzenberg, T. Nilsson, G. Nyman, R. Palit, S. Paschalis, W. Prokopowicz, R. Reifarth, A. Richter, K. Riisager, G. Schrieder, H. Simon, K. Sümmerer, O. Tengblad, H. Weick, and M. Zhukov, The unbound isotopes <sup>9,10</sup>He, Nucl. Phys. A 842, 15 (2010).
- [28] M. Vorabbi, A. Calci, P. Navrátil, M. K. G. Kruse, S. Quaglioni, and G. Hupin, Structure of the exotic <sup>9</sup>He nucleus from the no-core shell model with continuum, Phys. Rev. C 97, 034314 (2018).
- [29] M. Wallace, M. Famiano, M.-J. van Goethem, A. Rogers, W. Lynch, J. Clifford, F. Delaunay, J. Lee, S. Labostov, M. Mocko, L. Morris, A. Moroni, B. Nett, D. Oostdyk, R. Krishnasamy, M. Tsang, R. de Souza, S. Hudan, L. Sobotka, R. Charity, J. Elson, and G. Engel, The high resolution array (HiRA) for rare isotope beam experiments, Nucl. Instrum. Methods Phys. Res. A 583, 302 (2007).
- [30] See Supplemental Material at [URL inserted by publisher] for more details on experiment, data analysis, and theory calculations, and the list of the predicted states; it includes Refs. [3, 7, 22, 31, 41, 42, 45, 53–56].
- [31] T. B. Webb, R. J. Charity, J. M. Elson, D. E. M. Hoff, C. D. Pruitt, L. G. Sobotka, K. W. Brown, J. Barney, G. Cerizza, J. Estee, G. Jhang, W. G. Lynch, J. Manfredi, P. Morfouace, C. Santamaria, S. Sweany, M. B. Tsang, T. Tsang, S. M. Wang, Y. Zhang, K. Zhu, S. A. Kuvin, D. McNeel, J. Smith, A. H. Wuosmaa, and Z. Chajecki, Particle decays of levels in <sup>11,12</sup>N and <sup>12</sup>O investigated with the invariant-mass method, Phys. Rev. C 100, 024306 (2019).
- [32] T. B. Webb, R. J. Charity, J. M. Elson, D. E. M. Hoff, C. D. Pruitt, L. G. Sobotka, K. W. Brown, J. Barney, G. Cerizza, J. Estee, W. G. Lynch, J. Manfredi, P. Morfouace, C. Santamaria, S. Sweany, M. B. Tsang, T. Tsang, Y. Zhang, K. Zhu, S. A. Kuvin, D. McNeel, J. Smith, A. H. Wuosmaa, and Z. Chajecki, Invariantmass spectrum of <sup>11</sup>O, Phys. Rev. C 101, 044317 (2020).
- [33] T. B. Webb, S. M. Wang, K. W. Brown, R. J. Charity, J. M. Elson, J. Barney, G. Cerizza, Z. Chajecki, J. Estee, D. E. M. Hoff, S. A. Kuvin, W. G. Lynch, J. Manfredi, D. McNeel, P. Morfouace, W. Nazarewicz, C. D. Pruitt, C. Santamaria, J. Smith, L. G. Sobotka, S. Sweany, C. Y. Tsang, M. B. Tsang, A. H. Wuosmaa, Y. Zhang, and K. Zhu, First observation of unbound <sup>11</sup>O, the mirror of the halo nucleus <sup>11</sup>Li, Phys. Rev. Lett. **122**, 122501 (2019).
- [34] R. J. Charity, T. B. Webb, J. M. Elson, D. E. M. Hoff, C. D. Pruitt, L. G. Sobotka, P. Navrátil, G. Hupin, K. Kravvaris, S. Quaglioni, K. W. Brown, G. Cerizza, J. Estee, W. G. Lynch, J. Manfredi, P. Morfouace, C. Santamaria, S. Sweany, M. B. Tsang, T. Tsang,

- K. Zhu, S. A. Kuvin, D. McNeel, J. Smith, A. H. Wuosmaa, and Z. Chajecki, Using spin alignment of inelastically excited nuclei in fast beams to assign spins: The spectroscopy of <sup>13</sup>O as a test case, Phys. Rev. C **104**, 024325 (2021).
- [35] R. J. Charity, T. B. Webb, L. G. Sobotka, and K. W. Brown, Spectroscopy of <sup>10</sup>N with the invariant-mass method, Phys. Rev. C 104, 054307 (2021).
- [36] N. Michel, W. Nazarewicz, M. Płoszajczak, and K. Bennaceur, Gamow shell model description of neutron-rich nuclei, Phys. Rev. Lett. 89, 042502 (2002).
- [37] N. Michel, W. Nazarewicz, M. Płoszajczak, and T. Vertse, Shell model in the complex energy plane, J. Phys. G 36, 40 (2009).
- [38] N. Michel and M. Płoszajczak, Gamow Shell Model: The Unified Theory of Nuclear Structure and Reactions, Vol. 983 (Springer, Cham, Switzerland, 2021).
- [39] J. Wylie, J. Okołowicz, W. Nazarewicz, M. Płoszajczak, S. M. Wang, X. Mao, and N. Michel, Phys. Rev. C 104, L061301 (2021).
- [40] Y. Jaganathen, R. M. I. Betan, N. Michel, W. Nazarewicz, and M. Płoszajczak, Quantified Gamow shell model interaction for psd-shell nuclei, Phys. Rev. C 96, 054316 (2017).
- [41] X. Mao, J. Rotureau, W. Nazarewicz, N. Michel, R. M. I. Betan, and Y. Jaganathen, Gamow-shell-model description of Li isotopes and their mirror partners, Phys. Rev. C 102, 24309 (2020).
- [42] S. M. Wang, W. Nazarewicz, R. J. Charity, and L. G. Sobotka, Structure and decay of the extremely proton-rich nuclei <sup>11,12</sup>O, Phys. Rev. C 99, 054302 (2019).
- [43] S. M. Wang and W. Nazarewicz, Fermion pair dynamics in open quantum systems, Phys. Rev. Lett. 126, 142501 (2021).
- [44] T. Myo, M. Odsuren, and K. Katō, Five-body resonances in <sup>8</sup>He and <sup>8</sup>C using the complex scaling method, Phys. Rev. C 104, 044306 (2021).
- [45] A. M. Lane and R. G. Thomas, R-matrix theory of nuclear reactions, Rev. Mod. Phys. 30, 257 (1958).

- [46] P. Bevington and D. Robinson, Data reduction and error analysis for the physical sciences (McGraw-Hill, Boston, 2003).
- [47] R. Andrae, T. Schulze-Hartung, and P. Melchior, Dos and don'ts of reduced χ-squared (2010), arXiv:1012.3754.
- [48] M. A. Stephens, EDF statistics for goodness of fit and some comparisons, J. Am. Stat. Assoc. **69**, 730 (1974).
- [49] K. Fossez, J. Rotureau, and W. Nazarewicz, Energy spectrum of neutron-rich helium isotopes: Complex made simple, Phys. Rev. C 98, 061302 (2018).
- [50] N. Michel, W. Nazarewicz, M. Płoszajczak, and J. Rotureau, Antibound states and halo formation in the gamow shell model, Phys. Rev. C 74, 054305 (2006).
- [51] A. I. Baz', Y. B. Zel'dovich, and A. M. Perelomov, Scattering, reactions and decay in nonrelativistic quantum mechanics (Israel Program for Scientific Translation, Jerusalem, 1969).
- [52] M. Peshkin, A. Volya, and V. Zelevinsky, Nonexponential and oscillatory decays in quantum mechanics, Europhys. Lett. 107, 40001 (2014).
- [53] R. J. Charity, K. W. Brown, J. Elson, W. Reviol, L. G. Sobotka, W. W. Buhro, Z. Chajecki, W. G. Lynch, J. Manfredi, R. Shane, R. H. Showalter, M. B. Tsang, D. Weisshaar, J. Winkelbauer, S. Bedoor, D. G. McNeel, and A. H. Wuosmaa, Invariant-mass spectroscopy of <sup>18</sup>Ne, <sup>16</sup> O, and <sup>10</sup>C excited states formed in neutron-transfer reactions, Phys. Rev. C 99, 044304 (2019).
- [54] I. A. Egorova, R. J. Charity, L. V. Grigorenko, Z. Chajecki, D. Coupland, J. M. Elson, T. K. Ghosh, M. E. Howard, H. Iwasaki, M. Kilburn, J. Lee, W. G. Lynch, J. Manfredi, S. T. Marley, A. Sanetullaev, R. Shane, D. V. Shetty, L. G. Sobotka, M. B. Tsang, J. Winkelbauer, A. H. Wuosmaa, M. Youngs, and M. V. Zhukov, Democratic decay of <sup>6</sup>Be exposed by correlations, Phys. Rev. Lett. 109, 202502 (2012).
- [55] R. J. Charity, L. G. Sobotka, T. B. Webb, and K. W. Brown, Two-proton decay from α-cluster states in <sup>10</sup>C and <sup>11</sup>N, Phys. Rev. C 105, 014314 (2022).
- [56] (2022), evaluated Nuclear Structure Data File (ENSDF), http://www.nndc.bnl.gov/ensdf/.